



## **RESEARCH ARTICLE**

# A Model of High-Speed Endovascular Sonothrombolysis with Vortex Ultrasound-Induced Shear Stress to Treat Cerebral Venous Sinus Thrombosis

Bohua Zhang<sup>1\*</sup>, Huaiyu Wu<sup>1\*</sup>, Howuk Kim<sup>1,2\*</sup>, Phoebe J. Welch<sup>3</sup>, Ashley Cornett<sup>4</sup>, Greyson Stocker<sup>4</sup>, Raul G. Nogueira<sup>5</sup>, Jinwook Kim<sup>6</sup>, Gabe Owens<sup>4</sup>, Paul A. Dayton<sup>6</sup>, Zhen Xu<sup>4</sup>, Chengzhi Shi<sup>3,7†</sup>, and Xiaoning Jiang<sup>1†</sup>

<sup>1</sup>Department of Mechanical & Aerospace Engineering, North Carolina State University, Raleigh, NC, USA. <sup>2</sup>Department of Mechanical Engineering, Inha University, Incheon, Republic of Korea. <sup>3</sup>George W. Woodruff School of Mechanical Engineering, Georgia Institute of Technology, Atlanta, GA, USA. <sup>4</sup>Department of Biomedical Engineering, University of Michigan, Ann Arbor, MI, USA. <sup>5</sup>Department of Neurology, University of Pittsburgh Medical Center, Pittsburgh, PA, USA. <sup>6</sup>Department of Biomedical Engineering, University of North Carolina, Chapel Hill, NC, USA. <sup>7</sup>Parker H. Petit Institute for Bioengineering and Bioscience, Georgia Institute of Technology, Atlanta, GA, USA.

\*Address correspondence to: chengzhi.shi@gatech.edu (C.S), xjiang5@ncsu.edu (X.J.) †These authors contributed equally to this work.

This research aims to demonstrate a novel vortex ultrasound enabled endovascular thrombolysis method designed for treating cerebral venous sinus thrombosis (CVST). This is a topic of substantial importance since current treatment modalities for CVST still fail in as many as 20% to 40% of the cases, and the incidence of CVST has increased since the outbreak of the coronavirus disease 2019 pandemic. Compared with conventional anticoagulant or thrombolytic drugs, sonothrombolysis has the potential to remarkably shorten the required treatment time owing to the direct clot targeting with acoustic waves. However, previously reported strategies for sonothrombolysis have not demonstrated clinically meaningful outcomes (e.g., recanalization within 30 min) in treating large, completely occluded veins or arteries. Here, we demonstrated a new vortex ultrasound technique for endovascular sonothrombolysis utilizing wavematter interaction-induced shear stress to enhance the lytic rate substantially. Our in vitro experiment showed that the lytic rate was increased by at least 64.3% compared with the nonvortex endovascular ultrasound treatment. A 3.1-g, 7.5-cm-long, completely occluded in vitro 3-dimensional model of acute CVST was fully recanalized within 8 min with a record-high lytic rate of 237.5 mg/min for acute bovine clot in vitro. Furthermore, we confirmed that the vortex ultrasound causes no vessel wall damage over exvivo canine veins. This vortex ultrasound thrombolysis technique potentially presents a new life-saving tool for severe CVST cases that cannot be efficaciously treated using existing therapies.

Citation: Zhang B, Wu H, Kim H, Welch PJ, Cornett A, Stocker G, Nogueira RG, Kim J, Owens G, Dayton P, Xu Z, Shi C, Jiang X. A Model of High-Speed Endovascular Sonothrombolysis with Vortex Ultrasound-Induced Shear Stress to Treat Cerebral Venous Sinus Thrombosis. Research 2023;6:Article 0048. https://doi.org/10.34133/research.0048

Submitted 31 October 2022 Accepted 22 December 2022 Published 9 February 2023

Copyright © 2023 Bohua Zhang et al. Exclusive Licensee Science and Technology Review Publishing House. No claim to original U.S. Government Works. Distributed under a Creative Commons Attribution License (CC BY 4.0).

## Introduction

Cerebral venous sinus thrombosis (CVST) is a pathologic blood clot formation in the cerebral venous sinuses, one of the most prevalent causes of stroke in young individuals [1,2]. The incidence of CVST has been reported as being between 2 and 13 per million per year in Europe [3–5]. More recent research reveals that the incidence of CVST is growing in the United States [6]. Over the last decade, there has been mounting evidence that early diagnosis and anticoagulant therapy minimize the morbidity and mortality associated with CVST [7]. It is common for CVST to lead to a breakdown of the blood-brain

barrier and a drop in cerebral perfusion pressure, which results in cerebral edema, local ischemia, and, in some cases, intracerebral hemorrhage (ICH) [1]. Although most patients respond favorably to existing treatments, some individuals fail to recover or continue to worsen despite receiving the best available treatments. The death rate for patients with CVST remains at approximately 10%, with yet another 10% of individuals receiving poor long-term prognoses [1]. Moreover, in contrast to most other types of strokes, which typically occur in older people, patients with CVST are much younger than the general population and are frequently pregnant women or young mothers who have recently given birth to a baby [1,8,9]. It is worth noting that a

statistically significant rise in the occurrence of CVST has indeed been reported during the coronavirus disease 2019 outbreak because of both the severe acute respiratory syndrome coronavirus 2 disease and the consequence of some vaccinations [10–18].

Currently, the 3 most common therapeutic options for CVST are systemic use of anticoagulants or thrombolytic medicines, decompressive craniectomy, and catheter-based endovascular therapy [1,19,20]. According to a recent randomized study, long-term anticoagulation failed to recanalize 33% and 40% of the patients receiving intravenous heparin accompanied by warfarin and dabigatran, respectively, despite the use of longterm anticoagulation for at least 5 months [21]. Decompressive craniectomy is a very invasive neurosurgical intervention consisting of partial skull removal, which, although potentially lifesaving, is often considered the last resource since it decompresses the edematous brain without addressing the underlying problem (e.g., occlusive venous clot) [19]. Thrombolytic medications such as tissue plasminogen activator (t-PA) destroy blood clots by dissolving the cross-linked fibrin proteins that form the structure of the clots [22]. Nevertheless, systemic fibrinolytic medications are frequently inefficient, require extended treatment periods (up to 16 h), and may result in severe hemorrhage in as many as 55% of patients, with around 10% of those instances resulting in possibly fatal ICH [1,23–26]. There have been a variety of catheter-based devices that may be used to treat clots in the target area, such as mechanical thrombectomy and catheter-directed administration of thrombolytic medicines. In severe CVST instances, mechanical thrombectomy is becoming more popular [27].

However, existing endovascular techniques are insufficiently successful because they are not specially intended to treat the venous sinus, which has an average diameter of more than 3 times greater than that of the intracranial arteries. Furthermore, those techniques provide a high probability of severe consequences, including vascular endothelial damage, which might result in deadly ICH [24,28]. When thrombolytic medications are delivered locally by catheter, the risks associated with systemic administration are reduced, and the drugs are more successful at delivering into the clot region. Despite this, the effectiveness of this approach is uncertain, and it is still associated with the concerns of ICH [22,23,28,29]. According to a newly published randomized clinical study, the inadequate efficiency of existing device technology is vividly highlighted by a limited group of participants (n = 33) compared to systemic anticoagulation (n = 34). Although endovascular therapy has a favorable safety record, the trial could not establish a therapeutic advantage [30]. The fact that preliminary randomized studies using the early thrombectomy technique failed to establish its effectiveness in arterial strokes, whereas later studies with second-generation arterial thrombectomy were resoundingly beneficial is noteworthy [31,32]. It is thus acceptable to speculate that, with new technical improvements, venous thrombectomy may one day be demonstrated to be advantageous in properly selected patients.

To overcome these constraints and enhance effective thrombus breakdown without raising the danger of cerebral or systemic hemorrhage consequences, ultrasound thrombolysis, also known as sonothrombolysis, has been explored [33]. The primary mechanisms involved in sonothrombolysis are the radiation force, acoustic streaming, and cavitation [34]. It has been discovered that fibrinolytic medications and contrast-agent-mediated ultrasound may speed up thrombolysis by increasing

the transport of drugs into the clot [34–37]. To improve the clot lysis efficiency, large aperture transducers were employed in conjunction with multifrequency excitations to maximize the acoustic cavitation effect [34,38-40]. Using a catheter-based ultrasound transducer (EKOS), a multicenter retrospective study found that ultrasound combined with t-PA shortened infusion time [41–43] and resulted in a higher rate of completely dissolving clots for deep venous thrombosis therapy [44,45]. Sonothrombolysis efficacy has been improved using microbubbles (MBs) and nanodroplets combined with forward-viewing transducers [46,47]. Clinical trials on the treatment of acute myocardial infarction, stroke, and deep vein thrombosis have demonstrated that ultrasound pulses with a high mechanical index (MI) and contrast agents are capable of reperfusion by clot dissolution and blood flow enhancement [48]. For instance, a recent study found that patients who received sonothrombolysis had substantially higher rates of reperfusion and asymptomatic intracerebral bleeding than those who received only intravenous thrombolysis [49]. Moreover, ultrasound applications such as transcranial colorcoded duplex sonography and intravascular ultrasound have been used to diagnose CVST in recent years [50-52]. However, there is currently no endovascular ultrasound catheter that can be used for CVST treatment because of the extended treatment period (>15 h) and the high t-PA dosage used (10 to 20 mg) [53], as well as the challenges related to the navigation into the more tortuous intracranial vessels. In addition, conventional sonothrombolysis therapies, mainly based on the mechanism of cavitation effects, often require a high peak negative pressure (PNP), which may be unsafe and challenging to accomplish in endovascular sonothrombolysis [54]. In this context, there is an unmet medical need for a thrombolysis strategy that can provide local, effective, and rapid lysis of various types of clots, such as large acute clots and completely occluded clots, while minimizing damage to the vessel and surrounding tissue, as well as many other medical symptoms related to high doses of drugs for CVST care.

Vortex ultrasound (also known as acoustic orbital angular momentum) is a form of the acoustic wave that propagates across space with a helical wavefront that rotates as it moves through the space [55]. Many acoustofluidic technologies have been developed on the basis of vortex acoustic waves to manipulate fluids and particles in a contact-free and biocompatible manner [56–58]. For example, acoustic tweezing techniques based on acoustic vortices can manipulate bioparticles across a broad range of size [59-61]. The vortex-ultrasound-induced shear force has the potential to break down clots safely and improve the efficacy of thrombolysis. The objective of this work is to demonstrate the endovascular vortex ultrasound (EVUS) thrombolysis (Fig. 1A) for safe and effective CVST treatment to achieve a substantial breakthrough in addressing the unmet medical sonothrombolysis challenges mentioned above [46,47]. A 2 by 2 array of 4 smallaperture, low-frequency (1.8 MHz) piezoelectric transducers (Fig. 1B), each with a forward-viewing surface that is shifted by a quarter wavelength along the wave propagation direction, can be patterned in this manner to produce a physical helical wavefront (Fig. 1C). The transducer array was assembled into a 9-French catheter (with the diameter of about 3.0 mm) combined with a lumen for cavitation agents and drug delivery (Fig. 1B). This study demonstrates for the first time that the vortex ultrasound mediated by the MBs induces localized shear stress to the blood clot (Fig. 1D) that is expected to increase the sonothrombolysis rate significantly. This new EVUS system enables effective and rapid treatment of large acute and fully occluded clots, thereby

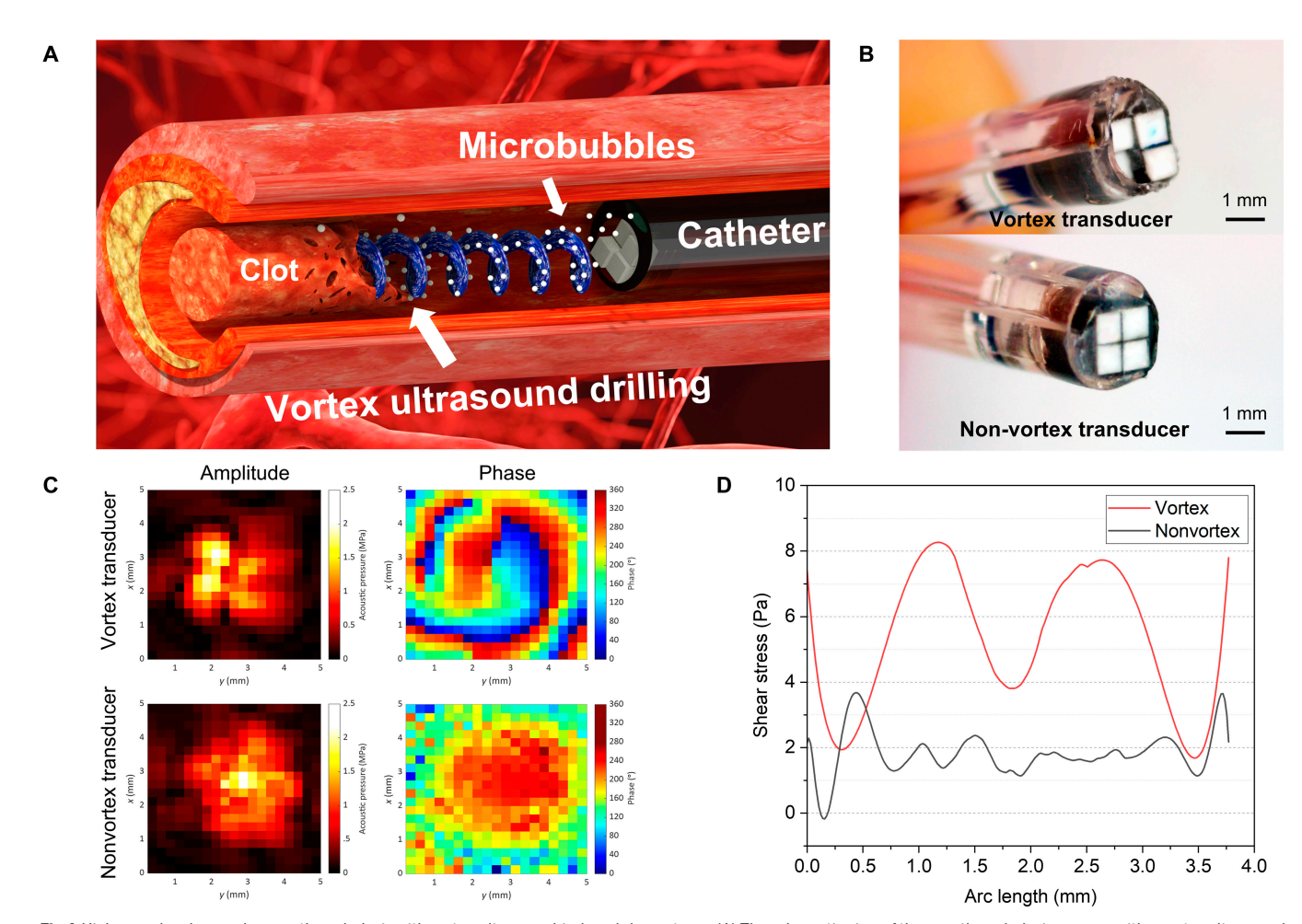


Fig.1. High-speed endovascular sonothrombolysis with vortex-ultrasound-induced shear stress. (A) The schematic view of the sonothrombolysis process with a vortex ultrasound transducer. The vortex ultrasound transducer is installed in a 9-French catheter and inserted into the blood vessel with a blood clot. The MB cavitation agents are injected through a drug delivery lumen of the catheter. The blood clot breaks up under the shear stress and cavitation effects of vortex ultrasound. (B) The prototype of the developed vortex transducer and nonvortex transducer installed in a 9-French catheter with drug delivery lumen. (C) The measured acoustic pressure map for vortex and nonvortex transducer. The phase map of the vortex transducer shows the swirling shape, and the nonvortex transducer only shows one circular shape. (D) The COMSOL calculated shear stress distribution in the blood clot along the azimuthal direction under the exposure of vortex and nonvortex ultrasound stimulation. The vortex ultrasound induces about 4-fold greater peak shear stress inside the blood clot than the nonvortex ultrasound.

significantly reducing damage to the vessel and surrounding tissue and shrinking the size of clot debris, reducing the risk of recurrent and distal embolisms.

# **Results**

#### Vortex ultrasound transducer

In this study, we leveraged the multilayer forward-viewing ultrasound transducer technology to develop a vortex ultrasound transducer array (Fig. 1B) to generate the helical wavefront (Fig. 1C). The 4 transducers were attached to an epoxy base containing air bubbles with a quarter wavelength (0.21 mm) step between neighboring transducers to form a 2 by 2 helical-patterned transducer array (Fig. S1A) for vortex ultrasound generation. Each transducer had an aperture of  $0.8 \times 0.8 \text{ mm}^2$  and a longitudinal-excitation-mode resonance frequency of 1.8 MHz. Air bubbles were introduced into the epoxy substrate to improve the acoustic contrast on the rear sides of the transducers and the forward ultrasonic emission. The transducer array prototype had an overall aperture of about  $1.65 \times 1.65 \text{ mm}^2$ . For MB and

lytic agent distribution, a 9-French 2-lumen catheter was used in conjunction with a duct channel explicitly designed for this purpose. Using a calibrated hydrophone, we measured the emitted acoustic pressure field of the prototyped transducer array. A pressure field was generated using a 60-V<sub>pp</sub> (peak-to-peak) input voltage and was measured both in amplitude and phase at a distance of approximately 1.5 wavelengths (1.2 mm) away from the transducer array (Fig. 1C). Noticeably, the pattern in the pressure amplitude was toroidal-like, as predicted for an acoustic vortex beam, and a spiral pattern was observed in the pressure phase. The vortex ultrasonic beam (insonation zone) diameter at -6 dB is about 2.3 mm, and it is predicted to be broader downstream because of diffraction as it propagates. The peak MI, a metric of measuring ultrasound bioeffects defined by the ultrasound beam's PNP divided by the square root of the operating frequency, achieved in the near field (0.5 wavelengths) of the transducer array is approximately 1.5, below the Food and Drug Administration's MI limit of 1.9 [62]. It is expected to be approximately 0.9 at about 1.5 wavelengths, which is sufficient to cause MB-mediated cavitation for enhanced sonothrombolysis while remaining safe for intravascular operation [46,47]. Compared to vortex ultrasound's spiral propagation pattern, an array of transducers with a flat front viewing surface generates a standard Gaussian beam profile (Fig. 1C), with the peak pressure amplitude located in the middle of the beam.

One of the most prominent advantages of vortex ultrasound is the strong in-plane pressure gradient that creates a rotational shearing stream in fluids [63] and considerable shear stress in the interacting solids when applied [64,65]. For rapid and safe CVST therapy, the induced shear stress in blood clots loosens and breaks the fibrins, increasing the sonothrombolysis rate and decreasing the necessary treatment time and lytic agent dosage. Numerical calculations performed using COMSOL Multiphysics revealed that the vortex ultrasound transducer induced larger shear stress along the azimuthal direction than conventional plane waves produced by nonvortex ultrasound transducer (Fig. 1D). On the basis of the simulation results, the Reynolds shear stress of the shear flow is around 80 dyne/cm<sup>2</sup>, which is close to the shear stress level in arterials vessels (10 to 70 dyne/cm<sup>2</sup>), but is about 10-fold larger than the shear stress in the venous vessels (1 to 6 dyne/cm<sup>2</sup>) [66-68]. This shear stress is much lower than the lowest recorded hemolysis threshold of 2,500 dyne/cm<sup>2</sup> in magnitude [69], which is confirmed by our hemolysis tests (Fig. S8). Thus, the shear stress induced by the vortex ultrasound has no potential to cause damage to the blood cells.

# In vitro vortex sonothrombolysis

Because CVST is often associated with clots that are just a few hours to a few days old [70], termed acute to subacute clots, our in vitro studies were performed to determine the rate of sonothrombolysis of acute clots using the prototyped vortex ultrasound transducer. A comparison of in vitro thrombolysis therapy outcomes between nonvortex and vortex ultrasound transducer treatment was shown in Fig. 2. The results illustrate the clot reduction during the treatment in 5-min intervals (Fig. 2A), and the vortex transducer shows a significantly higher clot lysis speed than the nonvortex transducer for 30 min of sonothrombolysis treatment. Following the treatment, the residual blood was washed out with saline (Fig. 2B) to compare the results of nonvortex and vortex ultrasonic treatments performed at the same push-through force level (0.056  $\pm$  0.021 N; feed-in speed, 1.66 mm/min). As indicated by the horizontal white dashed lines, the vortex transducer recanalized the whole length of the 50-mm acute clot, but the nonvortex transducer achieved less than 50% of clot lysis within the 30-min treatment period and did not recanalize the blood vessel phantom (Fig. 2A).

Moreover, the top and bottom cross-sections of blood clots (Fig. 2B) from the vortex treatment showed that the vortex transducer created an opening in the clot with a width of  $3.6 \pm 0.3$  mm. To determine the clot lysis rate for each case, we measured the clot mass both before and after the treatment. For the percent mass reduction of the clot, the nonvortex transducer had a lysis rate of 1.57%/min, and the lysis rate of vortex-transducer-based thrombolysis was measured to be about 2.45%/min, showing a significant increase of 1.56-fold rate over the nonvortex transducer (Fig. 2C). Comparing clot lysis speed, the nonvortex-transducer-based thrombolysis yielded an absolute lysis rate of 32.8 mg/min. In contrast, the vortex transducer had an absolute lysis rate of 53.9 mg/min, suggesting a significant increase of 64.3% with the vortex sonothrombolysis (Fig. 2D).

The vortex and nonvortex transducers were operated with an 80-V  $_{pp}$  input voltage (PNP, 3.24  $\pm$  0.19 MPa), a duty cycle of 7.5%, and a pulse repetition frequency (PRF) of 10 kHz based on the optimized parameters. A relatively low duty cycle (~7.5%) was applied for the safety consideration in this work. The temperature increased around 0.4 °C for 30-min treatment (Fig. S12), and the hematoxylin and eosin (H&E) histology (Fig. S6) results showed no damage over the vessel structure.

## In vitro parameter optimization

Next, we performed the in vitro parameter study to optimize the ultrasound input parameters for efficient sonothrombolysis with a vortex ultrasound transducer (Fig. 3). First, the different input voltages with fixed PRF (200 Hz) and duty cycle (5%) were used as the input factor for the vortex ultrasound transducer treatment. The result showed that the percent mass reduction of the clot significantly increased from 33.7% to 85.6% with the increasing input voltage from 20 to 100  $V_{pp}$  (Fig. 3A). In addition, the clot lysis speed significantly increased from 23.5 mg/min to 59.7 mg/min as the input voltage increased from 20 to 100  $V_{pp}$  (Fig. 3D). Our earlier study demonstrated that greater input voltages could result in higher PNP and MI [46]. However, to keep the ultrasound transducer operating within a safe voltage range,  $100 \text{ V}_{pp}$  was applied as the maximum input voltage due to the ultrasound transducer material limitation (45% of the AC depoling voltage for PZT-5A ceramics). For the safety of the treatment [71], 80  $V_{pp}$  was selected as the optimal input voltage for this study.

Different duty cycles with fixed input voltage (60 V  $_{pp}$ ) and PRF (200 Hz) were tested (under same PRF but different burst cycles) as the next input factor for optimizing vortex ultrasound transducer treatment. The results illustrated that the percent mass reduction of the clot significantly increased from 42.6% to 79.2% when the duty cycles increased from 2.5% to 10% (Fig. 3B). The clot lysis speed also increased considerably from 29.1 to 54.1 mg/min as the duty cycles increased from 2.5% to 10% (Fig. 3E). Since higher duty cycles ( $\geq$ 10%) may induce additional safety risks such as heating effects [72], a duty cycle at 7.5% was selected as the optimal duty cycle for this study.

Third, we tested different PRFs with fixed input voltage  $(60 \, V_{pp})$  and duty cycle (5%) (under same duty cycles but different burst cycles) to optimize this input factor. The results demonstrate that the percent mass reduction of the clot first significantly decreased from 77.8% to 59.4% with the increase in PRF from 10 to 100 Hz and later significantly increased from 66.8% to 79.3% with the increase in PRF from 200 to 10 kHz but then dropped dramatically to 59.5% when PRF further increased to 100 kHz (Fig. 3C). Similar trends can be found in the clot lysis speed when the PRF is varied from 10 Hz to 100 kHz (Fig. 3F). The 10-Hz and 10-kHz cases outperformed other cases, which was possibly correlated with the timing of MBs' intact traveling, oscillations, and ruptures. We selected 10 kHz for further tests since a previous study showed that the combination of "short-burst cycles and higher PRF" suppressed ultrasound-induced heating compared to the combination of "long-burst cycles and lower PRF" while maintaining the same duty cycle [72].

Next, the different feed-in speeds were tested as the input factor. Feed-in speed is the rate at which the catheter was pushed through the occluded vessel. This study revealed that the percent mass reduction of the clot significantly increased from 49.8% to

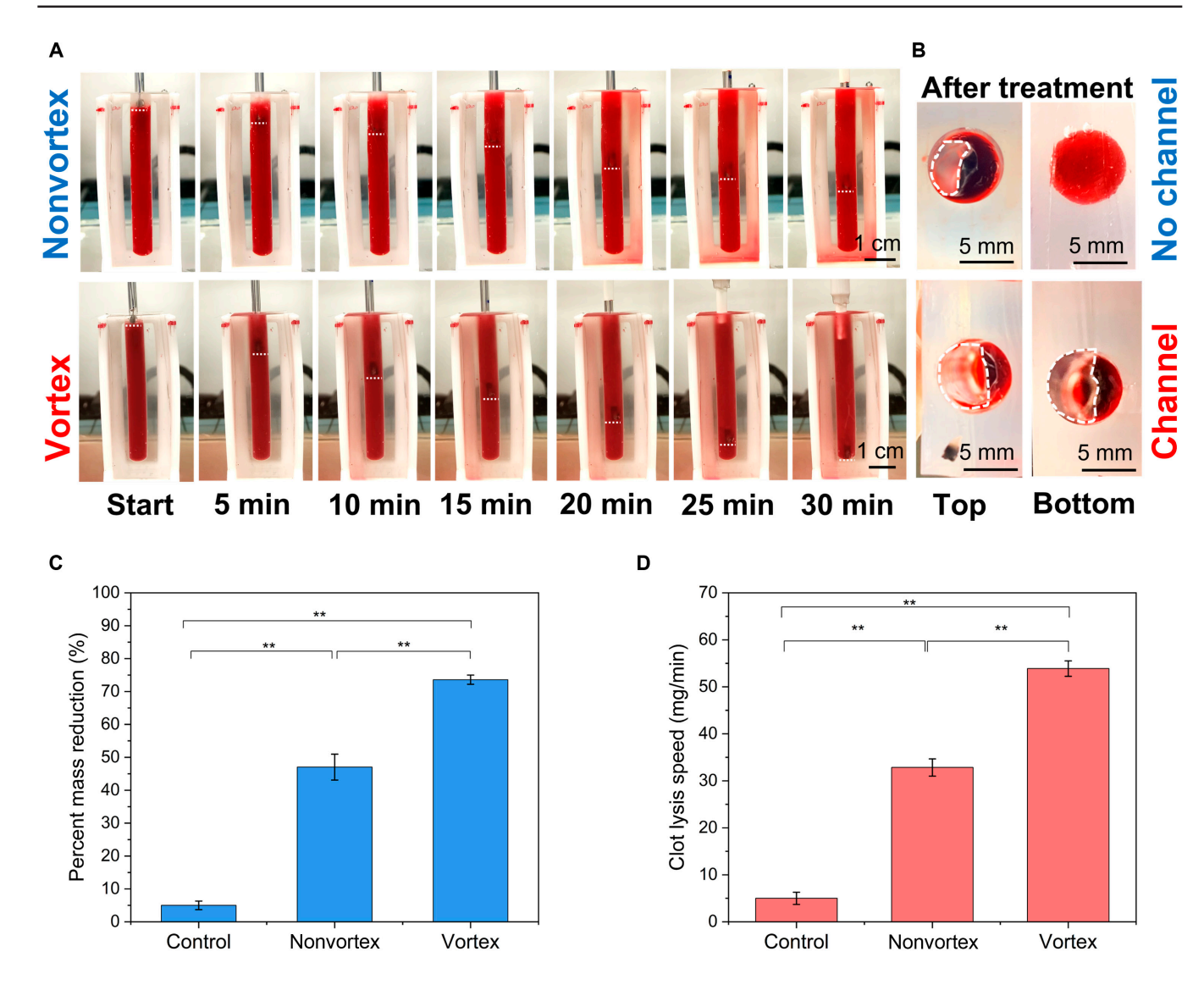


Fig. 2. The in vitro thrombolysis treatment results comparison for nonvortex and vortex ultrasound transducer treatments. (A) Thirty-minute treatment compared with the same level of push-through force. The horizontal white dashed lines mark the current location of the ultrasound transducer. During the 30-min treatment process, the vortex transducer exhibited a significantly higher clot lysis speed than the nonvortex transducer. (B) After 30-min treatment, the nonvortex transducer only treated about half of the blood clot (top channel opening size,  $10.2 \pm 0.7 \text{ mm}^2$ ), whereas the vortex ultrasound transducer formed a channel (flow channel opening size,  $23.5 \pm 0.8 \text{ mm}^2$ ) through the entire blood clot. (C) The percentage of the blood clot mass reduction comparison between the nonvortex and vortex transducer treatments. (D) The comparison of blood clot lysis speed between the nonvortex and vortex transducer treatments. (\*\*P < 0.01, n = 3)

79.6% when feed-in speed decreased from 10 to 1.66 mm/min (Fig. 3G). However, the clot lysis speed significantly decreased from 302.9 to 55.4 mg/min as the feed-in speed decreased from 10 to 1.66 mm/min (Fig. 3H). Although higher feed-in speed would significantly increase the clot lysis speed, it may also cause safety issues such as the large clot debris induced by fast mechanical push-through force. Therefore, the push-through force was measured under different feed-in speeds to determine the optimized parameter. These experiments demonstrated that the push-through forces with vortex ultrasound were about 4 times lower than the control group (without ultrasound) with different feed-in speeds (Fig. 3I), which proved the effectiveness of vortex ultrasound treatment. By overall consideration of the percent mass reduction (Fig. 3G) and clot lysis speed (Fig. 3H) while minimizing the induced push-through force (Fig. 3I), the feed-in

speed of 3.33 mm/min was selected as the optimal parameter for this study.

#### Cerebral venous sinus 3D model

An in vitro cerebral venous sinus 3-dimensional (3D) phantom flow model with an average sinus diameter of 10 mm was used to test the performance of the vortex transducer in treating CVST. The results showed that the completely occluded blood vessel was recanalized in only 8 min of treatment with a vortex ultrasound transducer (Fig. 4 and Movie S1). The measured clot mass before (3.1  $\pm$  0.3 g) and after (1.2  $\pm$  0.4 g) the treatment indicated that the vortex ultrasound transducer could achieve a high clot mass reduction rate (7.66%/min) and clot lysis speed (237.5 mg/min) in 8-min treatment, which is the significantly higher thrombolysis rate than the recent t-PA-free

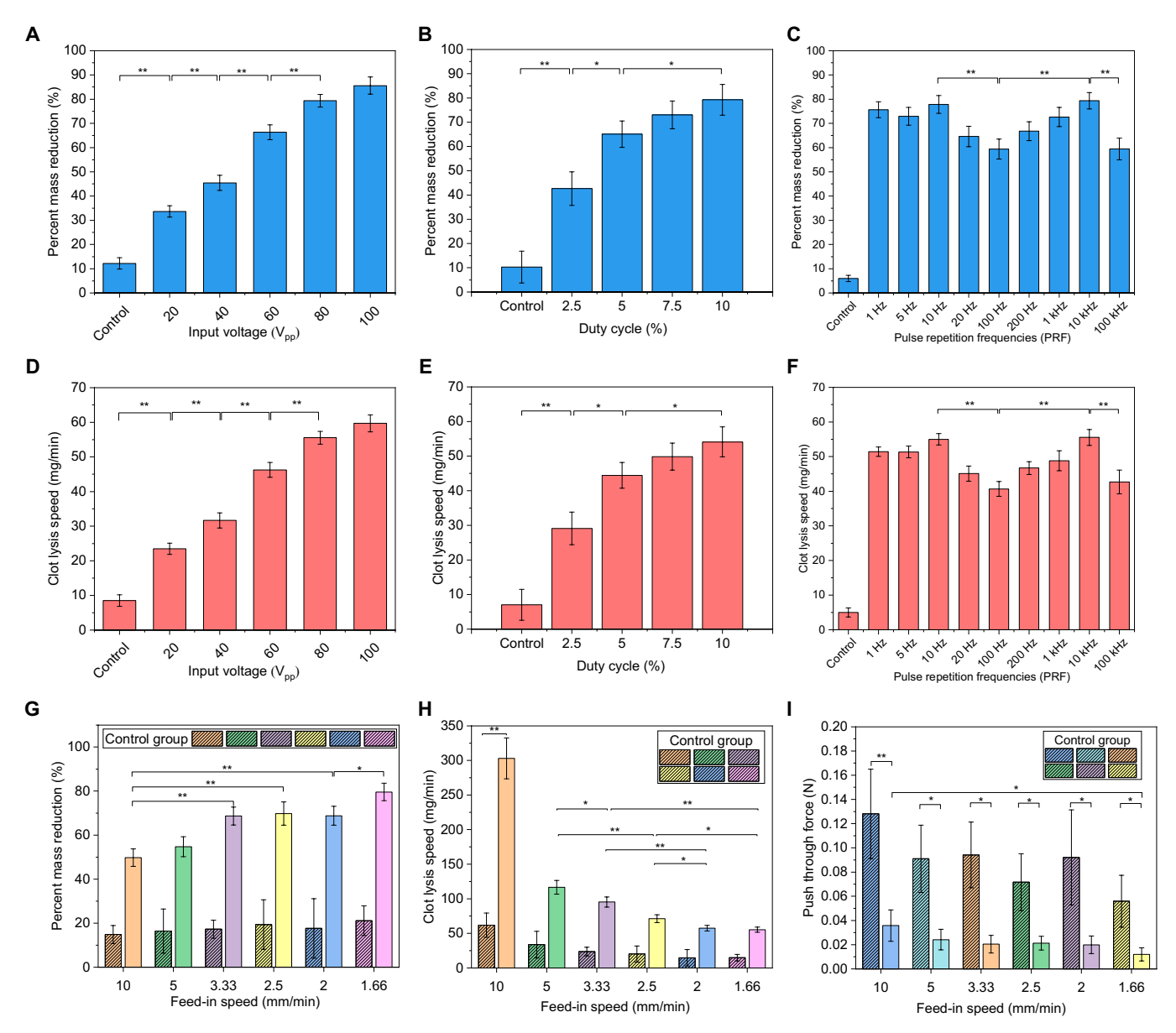


Fig. 3. The parameter study of in vitro sonothrombolysis with vortex ultrasound transducer treatment. (A) The percentage of blood clot mass reduction increases as input voltage increases from 20 to  $100 \text{ V}_{pp}$  (PRF, 200 Hz; duty cycle, 5%). The corresponding PNP value at different input voltages: 20, 40, 60, 80, and  $100 \text{ V}_{pp}$  was measured at about  $0.83 \pm 0.04$ ,  $1.66 \pm 0.08$ ,  $2.44 \pm 0.15$ ,  $3.24 \pm 0.19$ ,  $4.04 \pm 0.20$ , respectively. (B) The percentage of blood clot mass reduction increases as the duty cycle increases from 2.5% to 10% (input voltage,  $60 \text{ V}_{pp}$ ; PRF, 200 Hz). (C) The percentage of blood clot mass reduction varies with different PRFs. The percent mass reduction rate is highest when PRF is 10 and 10,000 Hz (input voltage,  $60 \text{ V}_{pp}$ ; duty cycle, 5%). (D) The lysis speed of blood clots increases with increasing input voltage. (E) The blood clot lysis speed increases as duty cycle increases from 2.5% to 10%. (F) The lysis speed of blood clots changes with different PRFs. (G) The percentage of blood clot mass reduction changes with different catheter feed-in speeds and significantly higher than controls across all feed-in speeds tested. (H) The lysis speed of blood clots changes with different catheter feed-in speeds. (I) The measured blood clot push-through force with different catheter feed-in speeds. The solid bar data present the vortex ultrasound treatment group. In contrast, the dashed bars denote the control group, which was only injected with saline without vortex ultrasound treatment. (\*P < 0.05, \*\*P < 0.01, n = 3)

endovascular sonothrombolysis (1.3% to 2.5%/min, 2 to 4.6 mg/min) [46,47,73–75]. Moreover, the clot debris analysis revealed that most of the clot debris particle sizes were less than 100  $\mu m$  (Fig. S5), which indicated a low risk of dangerous embolus formation. The histology results of the bovine blood vessel wall cross-sections after operating the catheters of the vortex, nonvortex, and control groups (Fig. S6B, C, and D, respectively) and pixel comparison results (Fig. S6E) confirmed the safety of the surrounding vessel and tissues of the vortex ultrasound treatment.

#### **Discussion**

Here, we demonstrate a novel EVUS system with a small aperture array that generates vortex ultrasound with a helical pattern to induce localized shear stress in the blood clot, which dramatically accelerates sonothrombolysis and lowers the necessary drug dose and MI for clot dissolution in an in vitro 3D model of acute CVST. This device was the first to incorporate the novel contrast-agent-mediated vortex ultrasound for clot-dissolving technology into a 9-French catheter device

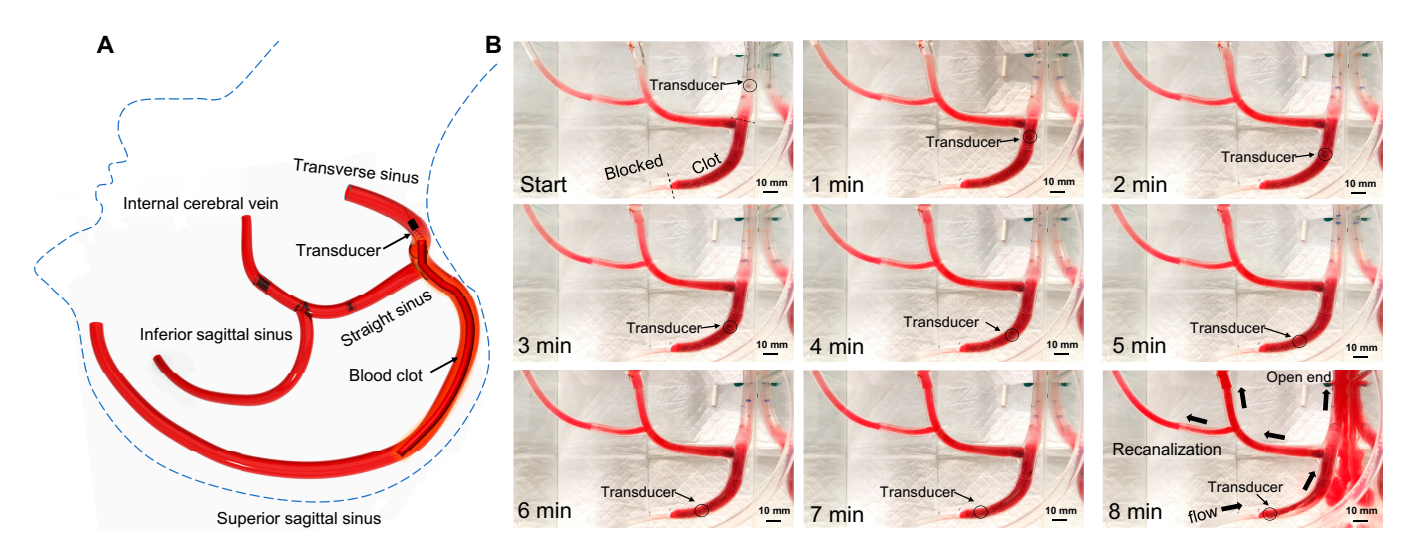


Fig. 4. The 3D phantom study of in vitro sonothrombolysis with vortex ultrasound transducer treatment. (A) Diagram of the cerebral venous sinus 3D phantom model with blood vessels labeled as well as the position of the blood clot, which runs along the superior sagittal sinus into the transverse sinus. The transducer starts in the transverse sinus. An outline of a human head and neck is included in the diagram, as indicated by the blue dashed line, to orient the position of these vessels in vivo. (B) A time lapse of the blood clot treatment (clot length,  $75 \pm 3$  mm; clot age, 1 h; treatment time, 8 min; vortex ultrasound transducer input factors; 80-V<sub>pp</sub> operating voltage; 7.5% duty cycle; frequency, 1.8 MHz; PRF, 10 kHz). Scale bars, 10 mm. The blood flow direction is marked by the thick black arrows in the final panel. The flow is driven by a pressure applied before and during the treatment to mimic the invivo environment. The location of the vortex transducer catheter tip is marked by the black circle in each panel.

to demonstrate the remarkably increased lytic efficiency and safety over existing thrombolysis approaches.

There is no endovascular thrombolysis technology currently available to treat severe CVST effectively. Therefore, this study developed a unique endovascular forward-viewing ultrasound transducer array with a helical pattern to generate vortex ultrasound in the cerebral venous sinus. For illustration, a 2 by 2 array of 4 multilayer stacked transducers (Fig. S1A) with resonance frequency at 1.8 MHz, with the forward viewing surfaces of neighboring transducers shifted by a quarter wavelength, has been used to induce a physical ultrasound phase delay, which is required to generate the helical wavefront of vortex ultrasound.

The vortex ultrasound produces an in-plane pressure gradient, which causes localized shear stress in the blood clot. The localized shear stress and cavitation-induced (Fig. S7) microstreaming significantly accelerate fibrinolysis in the clot, increasing the sonothrombolysis rate while simultaneously decreasing the medication dosage, PNP, and treatment duration. We hypothesize that the vortex-ultrasound-induced shear stress acts directly parallel to the clot front surface and mechanically disrupts the clot fibrin networks layer by layer to dissolve the clot more efficiently (Fig. S9). Besides, the shear stress induced by the vortex ultrasound loosens the clot structure, which improves the delivery of MBs and the lytic agent into the CVST. It should be pointed out that the induced shear stress would not present a hemolysis concern since the Reynolds shear stress of the shear flow is approximately 80 dynes/cm<sup>2</sup> from the simulation, which is significantly less than the lowest known hemolysis threshold (2,500 dynes/cm<sup>2</sup>) [69]. Besides, the in vitro hemolysis test results showed that the plasma-free hemoglobin level was about 5.7 to 23.4 mg/dl for 5- to 30-min treatment with vortex ultrasound and MBs (Fig. S8), which was significantly lower than the clinical signs of hemolysis (>40 mg/dl) [76] and treatment results from other technologies such as OmniWave (228 mg/dl), histotripsy (348  $\pm$  100 mg/dl) [77], and AngioJet (1367 mg/dl) [78]. For the first time, a low-frequency (1.8 MHz),

safe (MI, 0.5 to 1.5) vortex ultrasound beam was employed to achieve quick and safe catheter-directed CVST sonothrombolysis using a vortex ultrasound beam. Therefore, this study developed a unique, highly efficient, and safe sonothrombolysis approach as preclinical research, which will fulfill the therapeutic demands of patients with totally blocked, massive CVSTs in the future.

The other parameters that need to be considered in the future study are as follows: (a) Concentration of MBs: Concentration varied from  $10^6$  to  $10^9$  MBs/ml will be used for transducer operation parameters optimization. (b) Flow rate for MBs injection: Flow rate varied from 10 to 200  $\mu$ l/min will be used for the proposed transducer tests [which corresponds to approximately 100- to 5-min treatment durations, respectively, to stay within the indicated clinical doses (10  $\mu$ l/kg) of DEFINITY contrast agent for a 100-kg patient]. (c) Shear stress: The vortex-ultrasound-generated shear stress will be measured by the deformation of clot mimicking phantom gel on a micro strain gauge sensor. The operation parameters with the optimal shear stress will be chosen for high sonothrombolysis efficacy. (d) t-PA dose: t-PA concentration varied from 0.1 to 100  $\mu$ g/ml will be used for t-PA-mediated vortex ultrasound thrombolysis.

Many previous studies have shown that t-PA-mediated sonothrombolysis could significantly improve the clot lysis rate [47,79,80]. The main mechanism was based on stable cavitation, inertial cavitation, microstreaming, and acoustic radiation force to temporarily loosen fibrin clots and increase the diffusion of thrombolytic drugs into the blood clot [34,81,82]. For the shear-stress-induced thrombolysis, early study has discovered that an increase in shear rate generally promotes fibrin dissolving and that fibrin degraded by plasmin is abruptly dismantled by shear forces during the earliest stages of solubilization [83]. Prior research has demonstrated that the clot lysis rate is increased under higher shear stress (41 dyne/cm²) due to the increased delivery and refilling of drugs on the front surface of the clot, diffusion through the fibrin networks, and mechanical disruption of its 3D structure [84]. Moreover, the

shear stress induced by vortex ultrasound can be used to activate the shear-activated nanotherapeutics for targeted thrombolysis [85]. The combination of a vortex ultrasound platform with thrombolytic drugs such as t-PA is therefore anticipated to considerably enhance thrombolysis efficacy and will be investigated in future research.

The safety and efficacy need to be validated with more pre-clinical in vivo thrombolysis test before the clinical translation. To demonstrate the in vivo thrombolysis efficiency and safety of this platform, a swine CVST model with a vessel size (~6 mm) that mimics the size of the cerebral venous sinuses in humans (5 to 10 mm) will be developed in future study. However, there are some challenges that need to be addressed. For example, the effects of vortex ultrasound on the surrounding brain tissue and vascular wall and the recanalization efficacy need to be explored. The performance and bio-effects of clot disruption must be examined. The histological evaluation process and staining of the vascular injury should be established. For instance, microscopic examination of vein wall sections by H&E and Masson's trichrome stain should be used to assess cellular morphology and collagen deposition, respectively. Besides, any structural damage, hemorrhage, or inflammation of the vein wall needs to be examined. Moreover, the transducer design and catheter development need to be improved on the basis of the in vivo test results.

In summary, we described a novel vortex transducer technology specifically designed for the treatment of CVST. The developed vortex transducers showed an absolute lysis rate of 53.9 mg/min without parameter optimization, which is 64.3% higher than the lysis rate of nonvortex transducers (32.8 mg/ min) at the same push-through force level. For the optimized case, the improvement is expected to be even more remarkable. We demonstrated that the vortex ultrasound transducer could potentially fully recanalize the completely occluded acute CVST in vitro within 8 min of treatment and achieve a recordhigh clot lysis speed (237.5 mg/min). In severe cases of CVST and in patients with massive, fully blocked venous clots and who cannot be effectively treated with medications that are currently available, the vortex ultrasound thrombolysis technology may become a lifesaving treatment in the future. Additional studies using a novel CVST animal model are planned.

#### Methods

# **Transducer design**

The azimuthal polar coordinate of each transducer element is used to construct the vortex ultrasound transducer array to establish the suitable acoustic phase delay of each transducer element. The acoustic phase delay  $(\varphi)$  of an element with an in-plane azimuthal polar coordinate  $\theta$  is provided by  $\varphi = l\theta$  to create vortex ultrasound with topological charge *l* (a quantity that represents the angular momentum carried by the vortex wave) [86,87]. Topological charges of greater magnitude suggest the presence of a vortex wave with higher angular momentum and a larger aperture [86]. The 2 by 2 transducer array design (Fig. S1) can produce vortex ultrasound with  $l = \pm 1$ , allowing us to achieve the minimum aperture size possible with this configuration. In this scenario, the acoustic phase delay between adjoining transducers is  $\pi/2$ , which corresponds to a quarter wavelength shift in their forward viewing surfaces when compared to one another. By employing the epoxy base, it is

possible to align the 4 components with a quarter wavelength (0.21 mm for 1.8 MHz) shift between the forward viewing surfaces of adjoining transducers to achieve the desired result.

#### Transducer fabrication

The fabrication procedure for the proposed transducer arrays is shown in Fig. S2. In this study, 2 piezoelectric plates (for example, PZT-5A, with an area of  $6 \times 6 \text{ mm}^2$  and thickness of 200 μm) were bonded together using steel-reinforced epoxy (8265S, J-B Weld Company, Sulphur Springs, TX, USA) with a thickness of around 20 µm. A quarter-wavelength matching layer composed of an alumina powder/epoxy bond combination with an acoustic impedance of 5 to 6 MRayls was added to the front side of the device. An air bubble/epoxy composite backing was applied on the backside of the piezoelectric plates with a thickness of about 6 wavelengths (1.5 mm). By lapping with the backing layer, the aperture height of 4 piezoelectric multilayers that were integrated with the matching and the backing varied by a quarter wavelength. The bonded stacks were diced for an element aperture of approximately  $0.8 \times 0.8 \text{ mm}^2$  (DISCO 322, DISCO Hi-Tec America Inc., San Jose, CA), yielding 4 multilayered stacks with varying aperture heights. The multilayered stacks were bonded using an electrically nonconductive alumina/ epoxy composite. After utilizing epoxy to isolate unnecessary electrodes, the transducer electrodes were connected with a coaxial cable (5381-006, AWG 38, Hitachi Cable America Inc., Manchester, NH). The piezoelectric transducers were combined into a 2-lumen flexible catheter with a 9-French diameter; one lumen guided the transducer, while the other served as a flow channel for administering drugs and contrast agents. The catheter was composed of polyethylene, which allowed the 9-French catheter to be flexible enough to be directed into the cerebral venous sinus during the procedure.

#### Transducer characterization

Following fabrication, the electrical impedance spectrum (Fig. S10) was examined by measuring the resonance frequency of the device using an impedance analyzer (Agilent 4294A precision impedance analyzer, Agilent Technologies Inc., Santa Clara, CA, USA). The average electrical impedance of vortex transducer was about 200  $\Omega$  at 1.8 MHz measured in air and 210  $\Omega$  measured in water. The average electrical impedance of nonvortex transducer was about 195  $\Omega$  at 1.8 MHz measured in air and 205  $\Omega$  measured in water. The average dielectric loss at 1 kHz was about 10.25 mU for vortex transducer and 10.48 mU for the nonvortex transducer. The average capacitance was about 474.8 pF for vortex transducer and 468.15 pF for the nonvortex transducer. Using a calibrated needle hydrophone (HNA-0400, ONDA Corp., Sunnyvale, CA), the transducer array was installed on a computer-controlled 3-axis translational stage (Anet A8, Anet Technology Co. Ltd., Shenzhen, China) to characterize the acoustic waveform and pressure output (Fig. S3). Using a function generator (33250A, Agilent Technologies Inc., Santa Clara, CA), a sinusoidal pulse with 10 cycles every 10 µs was sent to an RF power amplifier (75A250A, AR, Souderton, PA). The signal was amplified before being sent into the developed transducer. The pulse-echo test was conducted using a square wave pulser/receiver (Olympus 5077PR, Olympus NDT Inc., Waltham, MA) (Fig. S11). The measured -6-dB bandwidth was 39.56% for the vortex transducer and 40.52% for the nonvortex transducer.

# **Acute clot preparation**

Bovine blood was used to prepare the acute clot in a manner similar to our previous study [46,47]. Initially, anticoagulated bovine blood (Lampire Biological Laboratories, Pipersville, PA, USA) containing acid citrate dextrose was combined with 2.75% calcium chloride (Thermo Fisher Scientific, Fair Lawn, NJ, USA) in a 10:1 ratio (100 ml of blood/10 ml of CaCl<sub>2</sub>) to form the blood mixture. Next, the blood mixture solution was added to the polydimethylsiloxane (PDMS) channel (diameter, 7 mm) to form the acute blood clots (length,  $50 \pm 3$  mm; diameter,  $7 \pm 0.5$  mm). For the 3D phantom in vitro study, the blood mixture solution was injected into the 3D phantom channel to form the acute clot. Finally, the acute blood clots were incubated in the water bath (PolyPro Bath, Model RS-PB-100, USA) at 37 °C for one hour before use.

# MB preparation

The MBs were prepared in-house as described in previous studies [46,88,89]. Briefly, lipid mixtures were created by combining 1,2-distearoyl-sn-glycero-3-phosphocholine (DSPC) and 1,2-distearoyl-*sn*-glycero-3-phosphoethanolamine-*N*-methoxy (polyethylene–glycol)-2000 (DSPE-PEG2000) at a 9:1 molar ratio (Avanti Polar Lipids, Alabaster, AL, USA) in a solution that also included propylene glycol at a concentration of 15% (v/v), glycerol at a concentration of 5% (v/v), and phosphate-buffered saline at a concentration of 80%. After that, aliquots of lipid solution measuring 1.5 ml each were transferred to glass vials measuring 3 ml, and the air headspace in each vial was replaced with decafluorobutane gas (Fluoromed, Round Rock, TX, USA). MBs containing decafluorobutane gas cores and phospholipid shells may spontaneously develop when agitation using a Vialmix device (Lantheus Medical Imaging, N. Billerica, MA, USA) is performed. Singleparticle optical methods (Accusizer 780, Particle Sizing Systems, Santa Barbara, CA, USA) were used to assess the concentration of MBs and their diameter. The average size of the MBs was 1.1 µm, and their concentration was 10<sup>10</sup>/ml in each vial. The MBs solution was then diluted into 10<sup>9</sup>/ml for each in vitro test.

# In vitro test preparation

For each in vitro treatment experiment, the acute blood clot was placed inside the PDMS channel. As shown in Fig. S4, the PDMS channel was fixed on the balance (SPX123, OHAUS, Parsippany, NJ, USA) that was connected to a computer for the push-through force measurement in real time. A 3D motion stage was used to control the catheter feed-in speed to maintain the distance between the clot and vortex ultrasound transducer, about 1.0 mm within the focal zone. The vortex ultrasound transducer was powered by a radio frequency power amplifier (amplify ratio, 53 dB; model: 75A250A, AR Inc., Souderton, PA, USA), while the input sine wave signal was generated by a function generator (model: 33250A, Agilent Technologies Inc., Loveland, CO, USA). The vortex and nonvortex transducers were operated with an 80-V<sub>pp</sub> input voltage, a duty cycle of 7.5%, and a PRF of 10 kHz. The input voltage, duty cycle, PRF, and feed-in speed for the optimal parameters study may vary according to the different experimental conditions. The MB solution with a concentration of 10<sup>9</sup>/ml was delivered through the catheter using a microfluid pump (DUAL-NE-1010-US, New Era Pump Systems Inc., Farmingdale, NY, USA) with an infusion rate of 0.1 ml/min. A clot sample with a length of about  $50 \pm 3$  mm and a weight of about  $1.6 \pm 0.4$  g was employed for

each test. The length of the remaining clots was measured every 5 min for a total of 30 min. Following the treatment, the lysis rate and speed were computed, and the channel width was evaluated to compare the efficacy of the vortex and nonvortex transducers in terms of channel width. The temperature variation in the clot area was measured by a thermocouple (Type K, Omega Engineering Inc, CT, USA) connected to a data acquisition module (OM-DAQ-USB-2401, Omega Engineering Inc, CT, USA) under 1-Hz sampling rate. The results showed that the temperature increased only ~0.4 °C during the 30-min treatment (Fig. S12). For the in vitro 3D phantom experiment (Fig. 4), an acute blood clot (diameter,  $10 \pm 2$  mm; length, 75  $\pm$  3 mm) was incubated in the phantom channel. The 3D printed phantom channel was filled with saline and maintained at a temperature of  $37.5 \pm 0.5$  °C. The saline was pumped from the reservoir to the 3D phantom venous flow model using a peristaltic pump, and a valve was utilized to modify the inlet flow speed and liquid pressure. The fluid pressure was measured with a digital pressure gauge and maintained at 50.3 mm H<sub>2</sub>O by regulating the pumping speed and valve before the flow channel. The flowing outlet of the phantom channel was connected to a small water reservoir to collect the saline-containing clot fragments following thrombolysis treatment.

# **Vessel wall damage study**

To evaluate the vessel damage caused by sonothrombolysis treatment, we performed the ex vivo safety tests with vortex and nonvortex transducer using the Canine jugular veins (NC State College of Veterinary Medicine, Raleigh, USA). Before usage, canine jugular veins veins were kept in cold phosphate-buffered saline, and then the vessels were cleaned and trimmed to approximately 1 cm in length (Fig. S6A). After the split and mounted in a water tank with degas water, samples were treated in 3 groups with nonvortex ultrasound + MBs and vortex ultrasound + MBs, respectively. Each test takes 30 min with the standard ultrasound parameters for the sonothrombolysis. Another untreated sample from the same jugular vein was picked as the control group. The treated vessels were then clipped to isolate the region of excitation and fixed in formalin for histological examination.

H&E staining was performed for the 3 groups of samples. Three mirrored cross-sections were obtained for the sample at 100  $\mu m$  (Fig. S6). After that, the slides were scanned using the EVOS FL Auto system (EVOS FL Auto Imaging System, Life Technologies Corporation, Carlsbad, USA) with 20× magnification. For each group, 6 regions were randomly selected along with the cross-sectional view, and different pixels were picked with a binary threshold. The pixel ratios representing the red color and white color were averaged and compared for the 3 groups.

#### Clot debris study

To evaluate the clot debris induced by sonothrombolysis treatment, we collected the blood solution contained with clot debris after each treatment. The blood solution was filtered with nylon plastic mesh sizes of 100 and 50  $\mu m$  (Fig. S5). After being dried for at least 24 h, the meshes were examined under the microscope, and the clot debris particle size was estimated by ImageJ software (Rasband WS, ImageJ, US National Institutes of Health, Bethesda, MD, USA). A one-way analysis of variance (ANOVA) was conducted for statistical significance in clot particle diameter and variances, with a significance level of 0.05 used to determine statistical significance.

9

# **Acknowledgments**

We want to acknowledge SonoVascular Inc., for using the 2-lumen catheters. We also want to acknowledge Extracorporeal Life Support (ECLS) Lab from University of Michigan for hemoglobin tests. Funding: B.Z., H.K., H.W., and X.J. thank the support from the National Institutes of Health (grant numbers R01HL141967, R41HL154735, and R21EB027304). P.J.W. and C.S. thank the support from the National Science Foundation (grant number CMMI-2142555). **Author contributions:** B.Z., H.K., H.W., Z.X., C.S., and X.J. designed the research. B.Z., H.K., H.W., A.C., and G.S. performed the experiments. B.Z. and H.K. performed the simulations. B.Z., Z.X., G.O., C.S., and X.J. analyzed the data. B.Z. wrote the original draft. B.Z., H.W., P.J.W., J.K., Z.X., C.S., and X.J. wrote and edited revised drafts. C.S. and X.J. supervised the study. C.S., X.J., P.A.D., and Z.X. acquired the funding. All authors provided active and valuable feedback on the manuscript. **Competing interests:** X.J. has a financial interest in SonoVascular Inc. who licensed an intravascular sonothrombolysis technology from NC state. R.G.N. reports consulting fees for advisory roles with Anaconda, Biogen, Cerenovus, Genentech, Philips, Hybernia, Imperative Care, Medtronic, Phenox, Philips, Prolong Pharmaceuticals, Stryker Neurovascular, Shanghai Wallaby, Synchron, and stock options for advisory roles with Astrocyte, Brainomix, Cerebrotech, Ceretrieve, Corindus Vascular Robotics, Vesalio, Viz-AI, RapidPulse, and Perfuze. R.G.N. is one of the principal investigators of the "Endovascular Therapy for Low NIHSS Ischemic Strokes (ENDOLOW)" trial. Funding for this project is provided by Cerenovus. R.G.N. is an investor in Viz-AI, Perfuze, Cerebrotech, Reist/Q'Apel Medical, Truvic, Vastrax, and Viseon.

# **Data Availability**

All data used to evaluate the findings in the paper are present in the paper and/or the Supplementary Materials. Other relevant data are available from corresponding authors upon reasonable request.

# **Supplementary Materials**

Fig. S1. The design of vortex and nonvortex transducer.

Fig. S2. The fabrication process of vortex transducer.

Fig. S3. The measured PNP of vortex and nonvortex transducers.

Fig. S4. The in vitro experimental setup.

Fig. S5. The results of clot debris study.

Fig. S6. The histology results of the canine blood vessel wall cross-sections after operations of the vortex, nonvortex, and control groups.

Fig. S7. The MB cavitation comparison for vortex ultrasound and nonvortex ultrasound.

Fig. S8. The in vitro hemolysis test results under different treatment time (5, 15, and 30 min) with vortex ultrasound (frequency, 1.8 MHz; duty cycle, 7.5%; PRF, 10 kHz; input voltage,  $80\,V_{pp}$ ) and MBs ( $10^9\,$  MBs/ml) treatment.

Fig. S9. The hypothesis of clot lysis under vortex ultrasound induced shear stress.

Fig. S10. The measured electrical impedance response of the vortex and nonvortex transducer in air and water medium

Fig. S11. The pulse-echo test results of the (A) vortex and (B) nonvortex transducer.

Fig. S12. The measured results of temperature variations in the clot area using vortex ultrasound treatment.

Movie S1. The 3D phantom study of in vitro sonothrombolysis with vortex ultrasound transducer treatment.

## References

- Silvis SM, de Sousa DA, Ferro JM, Coutinho JM. Cerebral venous thrombosis. *Nat Rev Neurol*. 2017;13(9):555–565.
- 2. Capecchi M, Abbattista M, Martinelli I. Cerebral venous sinus thrombosis. *J Thromb Haemost*. 2018;16(1):1918–1931.
- 3. Coutinho JM, Zuurbier SM, Aramideh M, Stam J. The incidence of cerebral venous thrombosis: A cross-sectional study. *Stroke*. 2012;43(12):3375–3377.
- Devasagayam S, Wyatt B, Leyden J, Kleinig T. Cerebral venous sinus thrombosis incidence is higher than previously thought: A retrospective population-based study. *Stroke*. 2016;47(9):2180–2182.
- 5. Kristoffersen ES, Harper CE, Vetvik KG, Zarnovicky S, Hansen JM, Faiz KW. Incidence and mortality of cerebral venous thrombosis in a Norwegian population. *Stroke*. 2020;51(10):3023–3029.
- Otite FO, Patel S, Sharma R, Khandwala P, Desai D, Latorre JG, Akano EO, Anikpezie N, Izzy S, Malik AM, et al. Trends in incidence and epidemiologic characteristics of cerebral venous thrombosis in the United States. *Neurology*. 2020;95(16):e2200–e2213.
- Martinelli I, Passamonti SM, Rossi E, De Stefano V. Cerebral sinus-venous thrombosis. *Intern Emerg Med.* 2012;7(Suppl. 3): S221–S225
- 8. Saposnik G, Barinagarrementeria F, Brown RD Jr, Bushnell CD, Cucchiara B, Cushman M, deVeber G, Ferro JM, Tsai FY, American Heart Association Stroke Council and the Council on Epidemiology and Prevention. Diagnosis and management of cerebral venous thrombosis: A statement for healthcare professionals from the American Heart Association/American Stroke Association. Stroke. 2011;42(4):1158–1192.
- 9. Ferro JM, Aguiar de Sousa D. Cerebral venous thrombosis: An update. *Curr Neurol Neurosci Rep.* 2019;19:74.
- 10. Cavalcanti DD, Raz E, Shapiro M, Dehkharghani S, Yaghi S, Lillemoe K, Nossek E, Torres J, Jain R, Riina HA, et al. Cerebral venous thrombosis associated with COVID-19. *AJNR Am J Neuroradiol*. 2020;41:1370–1376.
- Goldberg MF, Goldberg MF, Cerejo R, Tayal AH. Cerebrovascular disease in COVID-19. AJNR Am J Neuroradiol. 2020;41:1170–1172.
- 12. Hernández-Fernández F, Sandoval Valencia H, Barbella-Aponte RA, Collado-Jiménez R, Ayo-Martín Ó, Barrena C, Molina-Nuevo JD, García-García J, Lozano-Setién E, Alcahut-Rodriguez C, et al. Cerebrovascular disease in patients with COVID-19: Neuroimaging, histological and clinical description. *Brain*. 2020;143:3089–3103.
- 13. Klein DE, Libman R, Kirsch C, Arora R. Cerebral venous thrombosis: A typical presentation of COVID-19 in the young. *J Stroke Cerebrovasc Dis.* 2020;29:104989.
- Abdalkader M, Shaikh SP, Siegler JE, Cervantes-Arslanian AM, Tiu C, Radu RA, Tiu VE, Jillella DV, Mansour OY, Vera V, et al. Cerebral venous sinus thrombosis in COVID-19 patients: A multicenter study and review of literature. *J Stroke Cerebrovasc Dis*. 2021;30(6):105733.

- 15. Beretta S, da Re F, Francioni V, Remida P, Storti B, Fumagalli L, Piatti ML, Santoro P, Cereda D, Cutellè C, et al. Case report: Concomitant massive cerebral venous thrombosis and internal iliac vein thrombosis related to paucisymptomatic COVID-19 infection. Front Neurol. 2021;12:622130.
- 16. See I, Su JR, Lale A, Woo EJ, Guh AY, Shimabukuro TT, Streiff MB, Rao AK, Wheeler AP, Beavers SF, et al. US case reports of cerebral venous sinus thrombosis with thrombocytopenia after Ad26.COV2.S vaccination, march 2 to April 21, 2021. *JAMA*. 2021;325:2448–2456.
- 17. Mehta PR, Apap Mangion S, Benger M, Stanton BR, Czuprynska J, Arya R, Sztriha LK. Cerebral venous sinus thrombosis and thrombocytopenia after COVID-19 vaccination-a report of two UK cases. *Brain Behav Immun*. 2021;95:514–517.
- Dakay K, Cooper J, Bloomfield J, Overby P, Mayer SA, Nuoman R, Sahni R, Gulko E, Kaur G, Santarelli J, et al. Cerebral venous sinus thrombosis in COVID-19 infection: A case series and review of the literature. J Stroke Cerebrovasc Dis. 2021;30.
- Bousser M-G, Ferro JM. Cerebral venous thrombosis: An update. *Lancet Neurol*. 2007;6:162–170.
- 20. Luo Y, Tian X, Wang X. Diagnosis and treatment of cerebral venous thrombosis: A review. *Front Aging Neurosci.* 2018;10:2.
- Ferro JM, Coutinho JM, Dentali F, Kobayashi A, Alasheev A, Canhão P, Karpov D, Nagel S, Posthuma L, Roriz JM, et al. Safety and efficacy of dabigatran Etexilate vs dose-adjusted warfarin in patients with cerebral venous thrombosis: A randomized clinical trial. *JAMA Neurol*. 2019;76:1457–1465.
- 22. Goldhaber SZ, Morrison RB, Cardiology patient pages. Pulmonary embolism and deep vein thrombosis. *Circulation*. 2002;106(12):1436–1438.
- 23. Hughes RE, Tadi P, Bollu PC. TPA Therapy. In: StatPearls [Internet]. 2022 Jul 4. Treasure Island (FL): StatPearls Publishing; 2022.
- Wolberg AS, Rosendaal FR, Weitz JI, Jaffer IH, Agnelli G, Baglin T, Mackman N. Venous thrombosis. *Nat Rev Dis Primers*. 2015;1:15006.
- 25. Einhäupl K, Bousser M-G, de Bruijn SFTM, Ferro JM, Martinelli I, Masuhr F, Stam J. EFNS guideline on the treatment of cerebral venous and sinus thrombosis. *Eur J Neurol.* 2006;13(6):553–559.
- 26. Viegas LD, Stolz E, Canhão P, Ferro JM. Systemic thrombolysis for cerebral venous and dural sinus thrombosis: A systematic review. *Cerebrovasc Dis.* 2014;37:43–50.
- Haghighi AB, Mahmoodi M, Edgell RC, Cruz-Flores S, Ghanaati H, Jamshidi M, Zaidat OO. Mechanical Thrombectomy for cerebral venous sinus thrombosis: A comprehensive literature review. *Clin Appl Thromb*. 2014;20(5):507–515.
- 28. Chatterjee S, Chakraborty A, Weinberg I, Kadakia M, Wilensky RL, Sardar P, Kumbhani DJ, Mukherjee D, Jaff MR, Giri J. Thrombolysis for pulmonary embolism and risk of all-cause mortality, major bleeding, and intracranial hemorrhage: A meta-analysis. *JAMA*. 2014;311:2414–2421.
- 29. Beckman MG, Hooper WC, Critchley SE, Ortel TL. Venous thromboembolism: A public health concern. *Am J Prev Med.* 2010;38(Suppl. 4):S495–S501.
- Coutinho JM, Zuurbier SM, Bousser MG, Ji X, Canhão P, Roos YB, Crassard I, Nunes AP, Uyttenboogaart M, Chen J, et al. Effect of endovascular treatment with medical management vs standard care on severe cerebral venous thrombosis: The TO-ACT randomized clinical trial. *JAMA Neurol*. 2020;77:966–973.

- 31. Nogueira RG, Gupta R, Dávalos A. IMS-III and SYNTHESIS expansion trials of endovascular therapy in acute ischemic stroke: How can we improve? *Stroke*. 2013;44:3272–3274.
- 32. Goyal M, Menon BK, van Zwam W, Dippel DW, Mitchell PJ, Demchuk AM, Dávalos A, Majoie CB, van der Lugt A, de Miquel MA, et al. Endovascular thrombectomy after largevessel ischaemic stroke: A meta-analysis of individual patient data from five randomised trials. *Lancet*. 2016;387:1723–1731.
- Francis CW, Suchkova VN. Ultrasound and thrombolysis. Vasc Med. 2001;6:181–187.
- Bader KB, Gruber MJ, Holland CK. Shaken and stirred: Mechanisms of ultrasound-enhanced thrombolysis. *Ultrasound Med Biol.* 2015;41:187–196.
- 35. Alexandrov AV, Mikulik R, Ribo M, Sharma VK, Lao AY, Tsivgoulis G, Sugg RM, Barreto A, Sierzenski P, Malkoff MD, et al. A pilot randomized clinical safety study of Sonothrombolysis augmentation with ultrasound-activated Perflutren-lipid microspheres for acute ischemic stroke. Stroke. 2008;39(5):1464–1469.
- 36. Barreto AD, Alexandrov AV, Shen L, Sisson A, Bursaw AW, Sahota P, Peng H, Ardjomand-Hessabi M, Pandurengan R, Rahbar MH, et al. CLOTBUST-hands free: Pilot safety study of a novel operator-independent ultrasound device in patients with acute ischemic stroke. *Stroke*. 2013;44:3376–3381.
- Eggers J, Ossadnik S, Seidel G. Enhanced clot dissolution in vitro by 1.8-MHz pulsed ultrasound. *Ultrasound Med Biol*. 2009;35:523–526.
- 38. Guo S, Jing Y, Jiang X. Temperature rise in tissue ablation using multi-frequency ultrasound. *IEEE Trans Ultrason Ferroelectr Freq Control*. 2013;60(8):1699–1707.
- Ma J, Guo S, Wu D, Geng X, Jiang X. Design, fabrication, and characterization of a single-aperture 1.5-MHz/3-MHz dualfrequency HIFU transducer. *IEEE Trans Ultrason Ferroelectr* Freq Control. 2013;60:1519–1529.
- Suo D, Guo S, Lin W, Jiang X, Jing Y. Thrombolysis using multi-frequency high intensity focused ultrasound at MHz range: An in vitro study. *Phys Med Biol*. 2015;60:7403–7418.
- 41. Atar S, Luo H, Nagai T, Sahm RA, Fishbein MC, Siegel RJ. Arterial thrombus dissolution in vivo using a transducertipped, high-frequency ultrasound catheter and local low-dose urokinase delivery. *J Endovasc Ther.* 2001;8(3):282–290.
- Siddiqi F, Odrljin TM, Fay PJ, Cox C, Francis CW. Binding of tissue-plasminogen activator to fibrin: Effect of ultrasound. *Blood*. 1998;91:2019–2025.
- 43. Schrijver AM, Reijnen MMPJ, van Oostayen JA, Hoksbergen AWJ, Lely RJ, van Leersum M, de Vries JPPM. Initial results of catheter-directed ultrasound-accelerated thrombolysis for thromboembolic obstructions of the aortofemoral arteries: A feasibility study. *Cardiovasc Intervent Radiol*. 2012;35:279–285.
- 44. Dumantepe M, Tarhan IA, Ozler A. Treatment of chronic deep vein thrombosis using ultrasound accelerated catheter-directed thrombolysis. *Eur J Vasc Endovasc Surg.* 2013;46:366–371.
- 45. Marmagkiolis K, Lendel V, Cilingiroglu M. EKOS<sup>TM</sup> ultrasound accelerated catheter directed thrombolysis for acutely occluded femoro-popliteal graft. *Cardiovasc Revasc Med*. 2014;15(1):43–45.
- Kim J, Lindsey BD, Chang WY, Dai X, Stavas JM, Dayton PA, Jiang X. Intravascular forward-looking ultrasound transducers for microbubble-mediated sonothrombolysis. *Sci Rep.* 2017;7(1):3454.
- 47. Goel L, Wu H, Zhang B, Kim J, Dayton PA, Xu Z, Jiang X. Nanodroplet-mediated catheter-directed sonothrombolysis of retracted blood clots. *Microsyst Nanoeng*. 2021;7:3.

- El Kadi S, Porter TR, Verouden NJW, van Rossum AC, Kamp O. Contrast ultrasound, Sonothrombolysis and Sonoperfusion in cardiovascular disease: Shifting to Theragnostic clinical trials. *JACC Cardiovasc Imaging*. 2022;15(2):345–360.
- 49. Li X, du H, Song Z, Wang H, Tan Z, Xiao M, Zhang F. Efficacy and safety of sonothrombolysis in patients with acute ischemic stroke: A systematic review and meta-analysis. *J Neurol Sci.* 2020;416:116998.
- 50. Stolz E, Kaps M, Kern A, Babacan SS, Dorndorf W. Transcranial color-coded duplex sonography of intracranial veins and sinuses in adults reference data from 130 volunteers. *Stroke*. 1999;30:1070–1075.
- 51. Stolz EP. Role of ultrasound in diagnosis and management of cerebral vein and sinus thrombosis. *Front Neurol Neurosci*. 2008;23:112–121.
- Alvis-Miranda HR, Castellar-Leones SM, Alcala-Cerra G, Moscote-Salazar LR. Cerebral sinus venous thrombosis. *J Neurosci Rural Pract*. 2013;4(4):427–438.
- 53. Owens CA. Ultrasound-enhanced thrombolysis: EKOS EndoWave infusion catheter system. *Semin Intervent Radiol*. 2008;25(1):37–41.
- 54. Bader KB, Bouchoux G, Holland CK. Sonothrombolysis. *Adv Exp Med Biol.* 2016;880:339–362.
- 55. Hefner BT, Marston PL. An acoustical helicoidal wave transducer with applications for the alignment of ultrasonic and underwater systems. *J Acoust Soc Am.* 1999;106:3313–3316.
- Rufo J, Cai F, Friend J, Wiklund M, Huang TJ. Acoustofluidics for biomedical applications. *Nat Rev Methods Prim*. 2022;2(1):30.
- 57. Mao Z, Li P, Wu M, Bachman H, Mesyngier N, Guo X, Liu S, Costanzo F, Huang TJ. Enriching nanoparticles via acoustofluidics. *ACS Nano*. 2017;11:603–612.
- 58. Gu Y, Chen C, Rufo J, Shen C, Wang Z, Huang PH, Fu H, Zhang P, Cummer SA, Tian Z, et al. Acoustofluidic holography for micro- to nanoscale particle manipulation. *ACS Nano*. 2020;14:14635–14645.
- 59. Ozcelik A, Rufo J, Guo F, Gu Y, Li P, Lata J, Huang TJ. Acoustic tweezers for the life sciences. *Nat Methods*. 2018;15:1021–1028.
- 60. Rufo J, Zhang P, Zhong R, Lee LP, Huang TJ. A sound approach to advancing healthcare systems: The future of biomedical acoustics. *Nat Commun*. 2022;13:3459.
- 61. Baudoin M, Gerbedoen JC, Riaud A, Matar OB, Smagin N, Thomas JL. Folding a focalized acoustical vortex on a flat holographic transducer: Miniaturized selective acoustical tweezers. *Sci Adv.* 2019;5:eaav1967.
- 62. Şen T, Tüfekçioğlu O, Koza Y. Mechanical index. *Anatol J Cardiol*. 2015;15(4):334–336.
- 63. Hong Z, Zhang J, Drinkwater BW. Observation of orbital angular momentum transfer from Bessel-shaped acoustic vortices to diphasic liquid-microparticle mixtures. *Phys Rev Lett.* 2015;114:214301.
- 64. Zhang L, Marston PL. Angular momentum flux of nonparaxial acoustic vortex beams and torques on axisymmetric objects. *Phys Rev E.* 2011;84(6):65601.
- Anhäuser A, Wunenburger R, Brasselet E. Acoustic rotational manipulation using orbital angular momentum transfer. *Phys Rev Lett.* 2012;109(3):34301.
- Malek AM, Alper SL, Izumo S. Hemodynamic shear stress and its role in atherosclerosis. *J Am Med Assoc*. 1999;282(21):2035–2042.

- 67. Nerem RM, Alexander RW, Chappell DC, Medford RM, Varner SE, Taylor WR. The study of the influence of flow on vascular endothelial biology. *Am J Med Sci.* 1998;316:169–175.
- 68. Ballermann BJ, Dardik A, Eng E, Liu A. Shear stress and the endothelium. *Kidney Int Suppl.* 1998;54:S100–S108.
- 69. Sutera SP, Mehrjardi MH. Deformation and fragmentation of human red blood cells in turbulent shear flow. *Biophys J*. 1975;15:1–10.
- Guenther G, Arauz A. Cerebral venous thrombosis: A diagnostic and treatment update. *Neurologia*. 2011;26:488–498.
- 71. Goel L, Wu H, Zhang B, Kim J, Dayton PA, Xu Z, Jiang X. Safety evaluation of a forward-viewing intravascular transducer for Sonothrombolysis: An in vitro and ex vivo study. *Ultrasound Med Biol.* 2021;47:3231–3239.
- Kim H, Wu H, Cho N, Zhong P, Mahmood K, Lyerly HK, Jiang X. Miniaturized Intracavitary forward-looking ultrasound transducer for tissue ablation. *IEEE Trans Biomed Eng.* 2020;67:2084–2093.
- 73. Zhang B, Wu H, Goel L, Kim H, Peng C, Kim J, Dayton PA, Gao Y, Jiang X. Magneto-sonothrombolysis with combination of magnetic microbubbles and nanodroplets. *Ultrasonics*. 2021;116:106487.
- 74. Wu H, Goel LD, Kim H, Zhang B, Kim J, Dayton PA, Xu Z, Jiang X. Dual-frequency intravascular Sonothrombolysis: An in vitro study. *IEEE Trans Ultrason Ferroelectr Freq Control*. 2021;68:3599–3607.
- 75. Kim H, Kim J, Wu H, Zhang B, Dayton PA, Jiang X. A multi-pillar piezoelectric stack transducer for nanodroplet mediated intravascular sonothrombolysis. *Ultrasonics*. 2021;116:106520.
- Katz JN, Jensen BC, Chang PP, Myers SL, Pagani FD, Kirklin JK. A multicenter analysis of clinical hemolysis in patients supported with durable, long-term left ventricular assist device therapy. *J Heart Lung Transplant*. 2015;34(5):701–709.
- Devanagondi R, Zhang X, Xu Z, Ives K, Levin A, Gurm H, Owens GE. Hemodynamic and hematologic effects of histotripsy of free-flowing blood: Implications for ultrasound-mediated thrombolysis. *J Vasc Interv Radiol*. 2015;26:1559–1565.
- 78. Lang EV, Kulis AM, Villani M, Barnhart W, Balano R, Cohen R. Hemolysis comparison between the OmniSonics OmniWave endovascular system and the Possis AngioJet in a porcine model. *J Vasc Interv Radiol*. 2008;19:1215–1221.
- 79. Holland CK, Vaidya SS, Datta S, Coussios C-C, Shaw GJ. Ultrasound-enhanced tissue plasminogen activator thrombolysis in an in vitro porcine clot model. *Thromb Res.* 2008;121:663–673.
- 80. Goel L, Wu H, Kim H, Zhang B, Kim J, Dayton PA, Xu Z, Jiang X. Examining the influence of low-dose tissue plasminogen activator on microbubble-mediated forward-viewing intravascular Sonothrombolysis. *Ultrasound Med Biol.* 2020;46:1698–1706.
- 81. Chuang Y-H, Cheng P-W, Chen S-C, Ruan J-L, Li P-C. Effects of ultrasound-induced inertial cavitation on enzymatic thrombolysis. *Ultrason Imaging*. 2010;32:81–90.
- Prokop AF, Soltani A, Roy RA. Cavitational mechanisms in ultrasound-accelerated fibrinolysis. *Ultrasound Med Biol*. 2007;33:924–933.
- 83. Komorowicz E, Kolev K, Léránt I, Machovich R. Flow rate–modulated dissolution of fibrin with clotembedded and circulating proteases. *Circ Res.* 1998;82(10):1102–1108.

- 84. Wootton DM, Popel AS, Alevriadou BR. An experimental and theoretical study on the dissolution of mural fibrin clots by tissue-type plasminogen activator. *Biotechnol Bioeng*. 2002;77(4):405–419.
- 85. Korin N, Kanapathipillai M, Matthews BD, Crescente M, Brill A, Mammoto T, Ghosh K, Jurek S, Bencherif SA, Bhatta D, et al. Shear-activated nanotherapeutics for drug targeting to obstructed blood vessels. *Science*. 2012;337(6095): 738–742.
- 86. Shi C, Dubois M, Wang Y, Zhang X. High-speed acoustic communication by multiplexing orbital angular momentum. *Proc Natl Acad Sci USA*. 2017;114(28):7250–7253.
- 87. Jiang X, Shi C, Wang Y, Smalley J, Cheng J, Zhang X. Nonresonant metasurface for fast decoding in acoustic communications. *Phys Rev Appl.* 2020;13(1):14014.
- 88. Shelton SE, Lindsey BD, Tsuruta JK, Foster FS, Dayton PA. Molecular acoustic angiography: A new technique for high-resolution superharmonic ultrasound molecular imaging. *Ultrasound Med Biol.* 2016;42:769–781.
- 89. Kim J, DeRuiter RM, Goel L, Xu Z, Jiang X, Dayton PA. A comparison of Sonothrombolysis in aged clots between low-boiling-point phase-change nanodroplets and microbubbles of the same composition. *Ultrasound Med Biol.* 2020;46:3059–3068.